

Cite this: *RSC Adv.*, 2017, **7**, 36382

## Improving interface adhesion of magnetic particle modified EVA hot melt adhesive through introduction of a thermodynamically compatible component

Xiaobin Lu,<sup>a</sup> Hongguo Zhao,<sup>b</sup> Chunhui Feng,<sup>c</sup> Qian Chen,<sup>d</sup> Zhao Zhang,<sup>a</sup> Chunhua Yang,<sup>a</sup> Xianru He<sup>ID \*a</sup> and Xin Wang<sup>\*a</sup>

In order to improve the compatibility of  $\text{Fe}_3\text{O}_4$  particles with ethylene vinyl acetate copolymers (EVA) composite hot melt adhesives (HMAs),  $\text{Fe}_3\text{O}_4$  magnetic particles were surface coated with polyvinyl acetate (PVAc). The PVAc-coated  $\text{Fe}_3\text{O}_4$  modified EVA composite HMAs were characterized by SEM, DSC, XRD, optical contact angle measuring, infrared dichroism and parallel-plate rheometer measurements. The results showed that  $\text{Fe}_3\text{O}_4$  particles were successfully coated by PVAc, leading to better dispersion of the particles in EVA composite HMAs. It was also found that the orientation structure, interfacial property and the flow properties of the modified HMAs were all changed, and the segment orientation degree and crystallinity of the modified EVA composite HMAs clearly increased with the increase of PVAc-coated  $\text{Fe}_3\text{O}_4$  particles content. Importantly, the peel strength of the modified HMAs was further enhanced. For the modified HMAs with 15 phr (parts per hundred resins) of PVAc-coated  $\text{Fe}_3\text{O}_4$  particles, the peel strength reached  $6.6 \text{ kN m}^{-1}$  and was increased by 247% compared with the unmodified HMAs.

Received 9th June 2017  
Accepted 15th July 2017

DOI: 10.1039/c7ra06467e  
[rsc.li/rsc-advances](http://rsc.li/rsc-advances)

### 1. Introduction

Hot melt adhesives (HMAs) are solid thermoplastic materials that have been used for a long time.<sup>1–3</sup> With the increasing demands of manufacturing, HMAs are widely used in packaging, product assembly, book binding, box and carton heat sealing as well as in other press-sensitive applications.<sup>4–7</sup> HMAs are often based on thermoplastic polymers. EVA copolymer is the most commonly used polymer in the HMAs industry.<sup>8–10</sup> The reason for this is largely because of the fact that EVA has a wide range of melt index values and good adhesion to a variety of materials, in addition to its low price. EVA composite HMAs have nonpolar polyethylene segments and polar vinyl acetate segments which can interact with polyethylene and iron based pipe, making them suitable for the fast repair of external anticorrosive polyethylene coating of oil and gas transportation pipelines.<sup>11,12</sup>

Despite all the advantages, in practice however, ordinary EVA composite HMAs could not reach industrial standards because

of their weak adhesion properties and poor processing fluidity. Effective ways of reinforcing the adhesion property and improving the fluidity of HMAs include using additives such as tackifiers and plasticizers, or blending the adhesives with different polymers. Takemoto<sup>13,14</sup> studied the effect of tackifiers on the adhesion properties of EVA copolymers and found that when the blends were miscible at testing temperature, the temperature at which the maximum of peel strength was found tended to increase with increasing content of tackifier. Park<sup>15,16</sup> studied the adhesion and viscoelastic properties of three EVA composite HMAs with different vinyl acetate contents (15–28 wt%) blended with three aromatic hydrocarbon resins of different softening points. Among all the researches, few have studied the action mechanism of inorganic particles on the peel strength of adhesives.

In our very first study,<sup>17</sup> inorganic magnetic  $\text{Fe}_3\text{O}_4$  nanoparticles were used to modify EVA composite HMAs through melt blending. It was found that the addition of  $\text{Fe}_3\text{O}_4$  nanoparticles could improve the interfacial adhesion properties of HMAs, as indicated by the increased peel strength of the products. General property-affecting factors to consider for particle-modified composites include particle size. Factors such as magnetic force are also critical considering the particle is magnetic. Thus, in our previous work,<sup>18</sup> we studied the effect of particle size and magnetic force of  $\text{Fe}_3\text{O}_4$  on various properties of the adhesive, particularly its peeling strength. Particle size

<sup>a</sup>School of Materials Science and Engineering, Southwest Petroleum University, Chengdu, China 610500. E-mail: [xrhe@swpu.edu.cn](mailto:xrhe@swpu.edu.cn); [xin.wang@swpu.edu.cn](mailto:xin.wang@swpu.edu.cn); Tel: +86 13981892993; +86 15680912015

<sup>b</sup>Petrochemical Research Institute, PetroChina, Lanzhou, China 730060

<sup>c</sup>Sichuan Guanya Science and Technology Co. Ltd, Nanchong, Sichuan, China 637500

<sup>d</sup>Nanchong Unicizers Chemical Industrial Co, Ltd, No. 150 Hexi Ave, Hexi Town, Jialing Dist, Nanchong, Sichuan, China 637000



ranges from four tenths of micros to micros were involved. Results showed that the influence of size for this system is somewhat different from the common knowledge, *i.e.* smaller size facilitates dispersion thus leads to better mechanical properties. The reduced magnetism associated with decreased particle size was found to account for the unusual phenomenon. Later in our studies,<sup>19,20</sup> several other approaches were employed to further improve the adhesion. Particularly, coupling with silane and plasma surface processing were compared. Though plasma processing was widely used in surface processing for its convenience and effectiveness, chemical modification using silane coupling agent was found to provide an enhanced interaction between the  $\text{Fe}_3\text{O}_4$  and EVA matrix, generating a significantly improved peeling strength of the adhesives. The previous works paved a way of the study of modified EVA hot melt adhesives using functional particles.

In the present manuscript, a total different idea was employed for the improvement of adhesion of EVA adhesives. Instead of functionally modifying the  $\text{Fe}_3\text{O}_4$  particles by such as silane coupling agents that provides added interactions between the particles and adhesives, this work involves a globular coating of PVAc, whose chemical structure is the same as the VAc components in EVA, on  $\text{Fe}_3\text{O}_4$  particles that chemically transforms the inorganic particles to an organic ingredient without sacrificing their magnetism (magnetic field is not blocked by polymer layer). The PVAc coating on the surface of  $\text{Fe}_3\text{O}_4$  is thermodynamically compatible with the VAc segments of EVA, which further enhances the interaction between the composite particles and the polar ingredient of the matrix, making the PVAc-PE polar-nonpolar chain in EVA orientation even more adequate than achieved with any of the approaches in our previous work. This gives an EVA composite hot melt adhesive with greatly improved adhesion on the metal-polymer interface. In order to study the mechanism of PVAc-coated  $\text{Fe}_3\text{O}_4$  particles on the improvement of the interfacial adhesion property of HMAs, the interfacial property, orientation structure, crystallization and flow property of HMAs were studied. In addition, the effect of PVAc-coated  $\text{Fe}_3\text{O}_4$  particles on the peel strength, segments orientation structure, crystallization and interfacial property as well as rheological properties were also studied.

## 2. Experimental section

### 2.1. Materials

EVA (VA content is about 28 wt%,  $M_w = 7.43 \times 10^4 \text{ g mol}^{-1}$ ,  $M_n = 2.72 \times 10^4 \text{ g mol}^{-1}$ ,  $M_w/M_n = 2.73$ ) block copolymer (industrial grade) was purchased from Honam Petrochemical Corp., South Korea. EVA (VA content is about 28 wt%) grafted maleic anhydride (EVA-g-MAH, industrial grade) was bought from Guangzhou Synthetic Chemical Factory, China. Colophony (industrial grade), paraffin wax (industrial grade), vinyl acetate (VAc, AR), sodium hydroxide (NaOH, AR), polyvinyl alcohol (PVA 1788, AR), ammonium persulfate (APS, AR), lauryl sodium sulfate (SDS, AR), oleic acid (OA, AR), emulsifier OP-10 (AR) and ethanol (AR) were all obtained from Chengdu Kelong Chemical Factory, China. Divinyl benzene (DVB, AR) and  $\text{Fe}_3\text{O}_4$  particles

(average particle size is 0.19  $\mu\text{m}$ ) were bought from Aladdin Industrial Corporation, China. Polyethylene (PE) heat shrinkable tape was supplied by China National Petroleum Corporation. Iron plates (X80 pipeline steel) of 20 mm wide, 3 mm thick and 150 mm long were custom made in the Metal Process Factory of South West Petroleum University, China. Deionized water was obtained from Water Purification System (UPZGK, Chengdu Ultrapure Technology Co., Ltd., PR China).

### 2.2. Sample preparation

**2.2.1. Surface pretreatment of  $\text{Fe}_3\text{O}_4$  particles.** The carboxyl group on oleic acid (OA) could form chemical bond with the hydroxyl group of  $\text{Fe}_3\text{O}_4$  particles on the surface, leading to the grafting of some OA molecule onto the  $\text{Fe}_3\text{O}_4$  particles surface. The OA-pretreated  $\text{Fe}_3\text{O}_4$  particles were prepared by the following method. 10 g of  $\text{Fe}_3\text{O}_4$  particles were dispersed in 350 mL of deionized water under ultrasonic, then 11 mL of OA were added at 0.5  $\text{mL min}^{-1}$  using a constant pressure funnel at 85 °C. The reaction was kept for 1 h under stirring at a speed of 350  $\text{rad min}^{-1}$  at 85 °C under nitrogen atmosphere. Last, the surface-pretreated particles were separated using magnet and washed with deionized water and ethanol for several times before drying in vacuum at 50 °C for 24 h.

**2.2.2. Preparation of PVAc-coated  $\text{Fe}_3\text{O}_4$  particles.** The PVAc surface coated  $\text{Fe}_3\text{O}_4$  particles were prepared *in situ* by emulsion polymerization. In brief, 25 g of the OA surface pretreated  $\text{Fe}_3\text{O}_4$  particles were first dispersed in 500 mL of PVA aqueous solution (4 wt%) through ultrasonic dispersion. Then 50 mL of vinyl acetate (VAc) monomer and composite emulsifier (4 g of op-10 and 2 g of SDS) were added to the above solution for pre-emulsification under nitrogen atmosphere. After 30 min, the system was heated to 75 °C and 20 wt% of the initiator (APS) was added. After another 30 min, the remaining 150 mL of VAc monomer was added to the emulsion, together with a 20 wt% of the initiator (APS). The rest of the initiator (60 wt%) was added every 30 min until finish, then 10 mL of divinyl benzene (DVB) was added to the emulsion. The total amount of the initiator (APS) was 1.2 g. The system was heated to 80 °C and kept for 1 h. Last, the PVAc-coated  $\text{Fe}_3\text{O}_4$  particles were separated, washed and dried in the same way as for OA-pretreated  $\text{Fe}_3\text{O}_4$  particles. The overall schematic for preparing surface coated magnetic particles was illustrated in Fig. 1.

**2.2.3. Preparation of PVAc-coated  $\text{Fe}_3\text{O}_4$  modified EVA composite HMAs.** PVAc-coated  $\text{Fe}_3\text{O}_4$  modified EVA composite HMAs were made up of 100 phr of EVA, 50 phr of colophony, 20 phr of paraffin wax and certain content of PVAc-coated  $\text{Fe}_3\text{O}_4$  particles varied from 0, 5, 10, 15, 20 to 25 phr. The preparation methods of composite HMAs were reported in our previous studies.<sup>18-20</sup> The peel test samples were prepared as follows. The composite HMAs were spread on a PE layer cut from PE heat shrinkable tape. The PE tape containing HMAs was pasted onto an iron plate with the HMAs still in molten state. After that the samples were pressed on a vulcanizing press under a pressure of 1 MPa at 60 °C for 2 h and then cooled at room temperature. All the test samples were processed at the same time with the same thermal stress history.



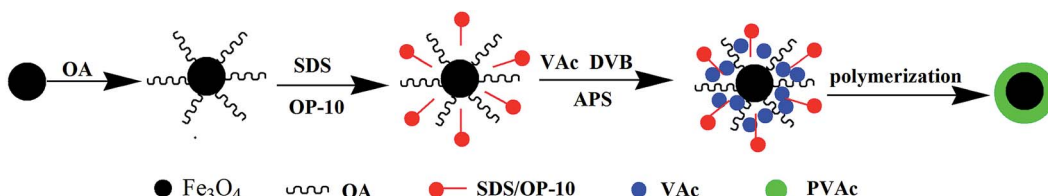


Fig. 1 Schematic illustration of preparing the PVAc-coated Fe<sub>3</sub>O<sub>4</sub> particles.

### 2.3. Characterization

**2.3.1. Scanning electron microscopy (SEM).** PVAc-coated Fe<sub>3</sub>O<sub>4</sub> particles were observed by a JSM-7500F SEM (Japan Electron Optics Laboratory). The surface and fractured surface of composite HMAs before peel test were also observed with this instrument.

**2.3.2. X-ray diffraction (XRD).** The crystal structure of particles was characterized by XRD (X Pert PRO MPD, PANalytical B.V., Netherlands) equipped with a Cu K $\alpha$  radiation ( $\lambda = 0.154$  nm) at diffraction angle ranged from 5 to 50° with a step size of 4° min<sup>-1</sup>.

**2.3.3. Vibrating sample magnetometer (VSM).** The saturated magnetic intensity of particles were measured by VSM (BKT-4500Z, Quantum Design Ltd, US) in an open circuit mode at 25 °C.

**2.3.4. Peel strength test.** The peel strength test was conducted based on the standard of GB/T2790-1995 of China at 25 °C and carried out on a microcomputer controlled electronic universal testing machine (CMT6104, Mechanical Testing & Simulation Systems, China). The peeling speed was 200 mm min<sup>-1</sup>. The test was repeated three times and the average value was obtained.

**2.3.5. Orientation degree test.** The orientation structure of composite HMAs was measured by infrared dichroism instrument (Nicolet 6700, Thermo Fisher Scientific, US) from 4000 to 500 cm<sup>-1</sup> with a resolution of 4 cm<sup>-1</sup>. The scanning frequency was 32. The thickness of samples were 10  $\mu$ m and the test angle was (0°, 90°), (10°, 100°), (20°, 110°), (30°, 120°), (40°, 130°) and (50°, 140°). The orientation degree  $R$  and relative orientation degree  $f'$  were obtained by eqn (1)–(3), respectively,<sup>21</sup>

$$R = A_{\alpha}/A_{\alpha+90} \quad (1)$$

$$f' = \frac{R - 1}{R + 2} \times \frac{2}{3 \cos^2 \alpha - 1} \quad (2)$$

$$f' = \frac{R - 1}{R + 2} \quad (3)$$

where  $R$  is the dichroic ratio,  $\alpha$  is the angle of molecular chain,  $A_{\alpha}$  is the absorption of infrared polarized light intensity at the angle of  $\alpha$ , and  $A_{\alpha+90}$  is the absorption of infrared polarized light intensity at the angle of  $\alpha + 90$ .

**2.3.6. Water contact angle test.** Water contact angle under ambient conditions were measured through sessile drop method with an optical contact angle measuring device (DSA30, Kruss, Germany) at 25 °C. The numerical value of the contact angle was determined by the tangent method and provided by the droplet shape analysis system software at a resolution of 0.01°.

**2.3.7. Crystallization test.** The crystallization of the composite HMAs was measured with a Mettler Toledo DSC823e differential scanning calorimetry. The sample was heated from 0 °C to 150 °C at a heating rate of 10 °C min<sup>-1</sup> under nitrogen atmosphere. Crystallinity of the composite HMAs was obtained from the DSC curves by calculating the percentage of the crystallization peak area among all peaks. The crystallinity was calculated by eqn (4),

$$W_c = \frac{\Delta H/m}{\Delta H_m^* \times 72\%} \times 100\% \quad (4)$$

where  $\Delta H_m^*$  is the melting enthalpy of unit mass of high-density polyethylene (292.6 J g<sup>-1</sup>),<sup>19</sup>  $\Delta H$  is the melting enthalpy of EVA composite HMAs,  $m$  is the mass of HMAs and 72% is the content of ethylene segments in EVA copolymer. The as obtained value of  $W_c$  includes the crystallinity of all PE segments in EVA adhesives and therefore is regarded as the relative crystallinity.

**2.3.8. Rheological property.** The viscoelasticity of composite HMAs was investigated on a Malvern Bohlin Gemini200 Parallel-plate rheometer at 75 °C with shear rate of 0.01 to 50 s<sup>-1</sup> in steady mode, and at a frequency from 0.01 to 100 Hz in dynamic mode. The specimen was a circular thin sheet of 5 mm thick with a diameter of 25 mm.

**2.3.9. Transmission electron microscopy (TEM).** The microstructure of the PVAc-coated Fe<sub>3</sub>O<sub>4</sub> particles were observed by a H-600 TEM (Hitachi limited corporation) with an accelerating voltage of 75 kV. The sample was prepared as

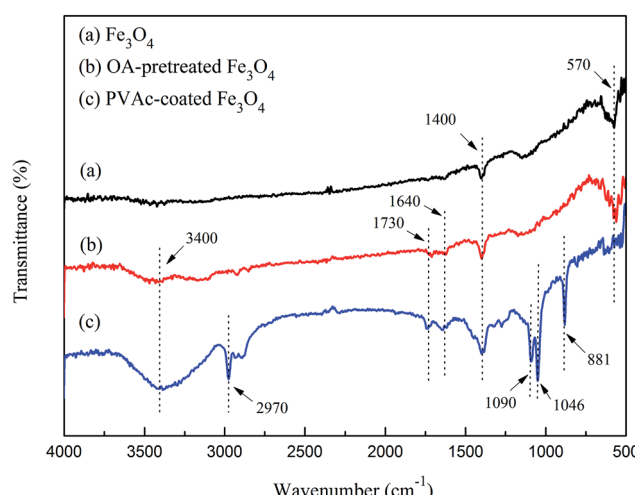


Fig. 2 FT-IR spectrograms of magnetic particles.

follows. A trace of the PVAc-coated  $\text{Fe}_3\text{O}_4$  were dispersed in deionized water through ultrasonic dispersion, then a drop of such liquid was dropped onto a copper grid and dyed by sulfuric acid.

#### 2.3.10. Fourier transform infrared spectroscopy (FT-IR).

The FT-IR spectrograms of  $\text{Fe}_3\text{O}_4$  and the modified  $\text{Fe}_3\text{O}_4$  particles at different modifications steps were carried out on a FT-IR (Nicolet 6700, Thermo Fisher Scientific Corp., Ltd., America) using KBr method.

#### 2.3.11. Thermo-gravimetric analysis (TGA).

The TGA curves of different  $\text{Fe}_3\text{O}_4$  particles and the EVA adhesives were tested on a TGA (TGA/SDTA85e, Mettler Toledo Corp., Ltd., Switzerland). The test range was from 40 °C to 700 °C with a heating rate of 10 °C min<sup>-1</sup> under the protection of nitrogen.

## 3. Results and discussion

### 3.1. Properties of PVAc-coated $\text{Fe}_3\text{O}_4$ particles

The absorption peaks at 570 cm<sup>-1</sup> and 1400 cm<sup>-1</sup> were the basic absorption peaks of  $\text{Fe}_3\text{O}_4$  particles,<sup>19</sup> as the infrared spectrograms shown in Fig. 2. For oleic acid (OA) pretreated  $\text{Fe}_3\text{O}_4$  (Fig. 2), the absorption peaks at 3400 cm<sup>-1</sup>, 1730 cm<sup>-1</sup> and 1640 cm<sup>-1</sup>

were the stretching vibration peak of -OH, C=O and -CH=CH<sub>2</sub> respectively,<sup>19,20</sup> which indicated that the oleic acid was grafted onto the surface of  $\text{Fe}_3\text{O}_4$  particles. Compared with OA-pretreated  $\text{Fe}_3\text{O}_4$ , for PVAc-coated  $\text{Fe}_3\text{O}_4$ , the new peaks at 2970 cm<sup>-1</sup> and the twin peaks at 1090 cm<sup>-1</sup> and 1046 cm<sup>-1</sup> were attributed to the vibration of -CH<sub>3</sub> and C-O in ester group, respectively,<sup>19</sup> and the peak at 881 cm<sup>-1</sup> was the basic peak of phenyl in DVB (Fig. 2), this all indicated that the PVAc was coated on  $\text{Fe}_3\text{O}_4$ .

The as-prepared PVAc-coated  $\text{Fe}_3\text{O}_4$  were spherical particles with a diameter of 0.31  $\mu\text{m}$ , which is larger than that of  $\text{Fe}_3\text{O}_4$  (0.19  $\mu\text{m}$ ), as shown in Fig. 3a and b. As the TEM micrographs of the PVAc-coated  $\text{Fe}_3\text{O}_4$  in Fig. 3(c) showed, the dark part was  $\text{Fe}_3\text{O}_4$  particles and the light-colored part on the edge was the organic PVAc coating. It is clear that  $\text{Fe}_3\text{O}_4$  particles were coated by a layer of organic coating. The TGA curves in Fig. 4 showed that  $\text{Fe}_3\text{O}_4$  had no obvious weight loss. In comparison, the OA-pretreated  $\text{Fe}_3\text{O}_4$  had about 8% of weight loss, while the PVAc-coated  $\text{Fe}_3\text{O}_4$  had about 30% of weight loss (Fig. 4). These are because the PVAc organic coating of PVAc-coated  $\text{Fe}_3\text{O}_4$  degraded at lower temperature and reduced the weigh retention. All these indicate that  $\text{Fe}_3\text{O}_4$  particles were successfully surface coated with a layer of PVAc polymer, resulting in an increased

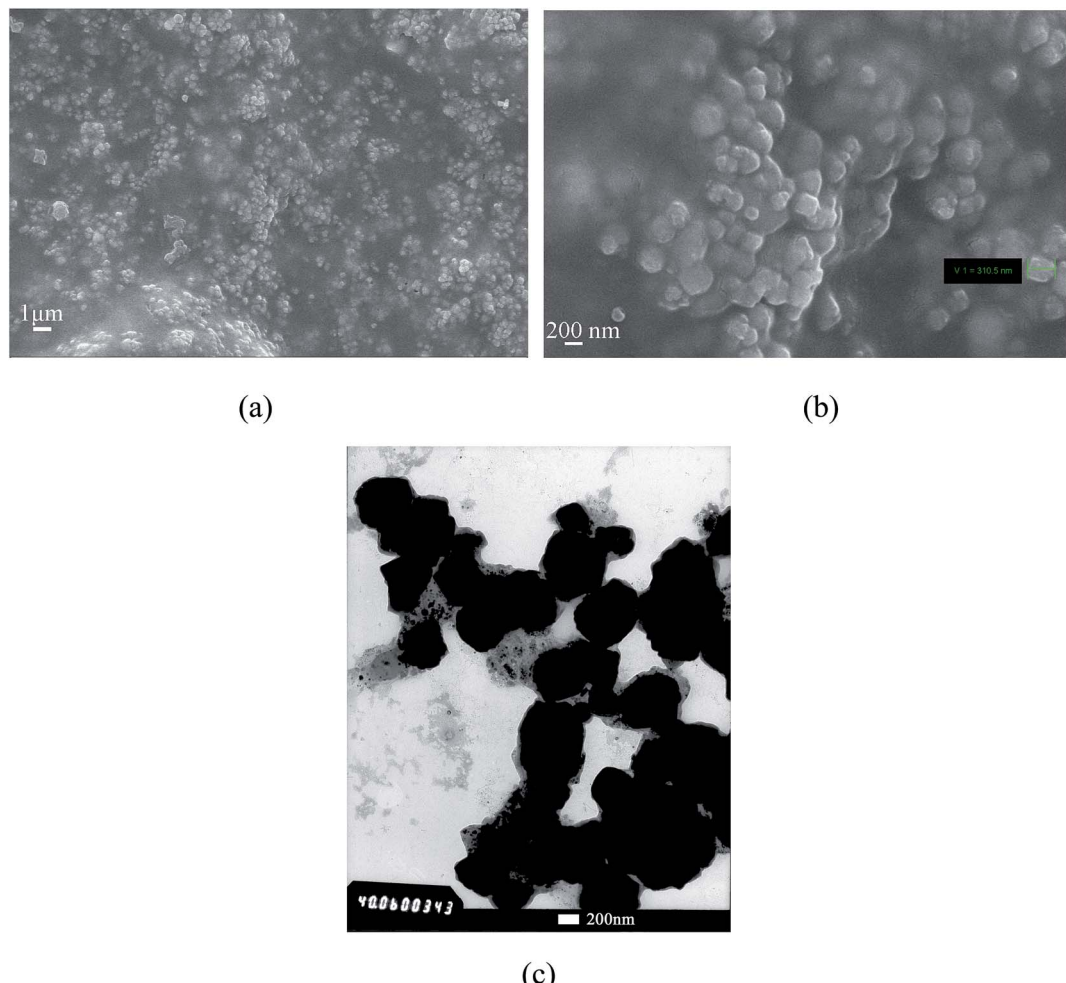


Fig. 3 (a, b) SEM micrographs and (c) TEM micrographs of PVAc-coated  $\text{Fe}_3\text{O}_4$  particles.



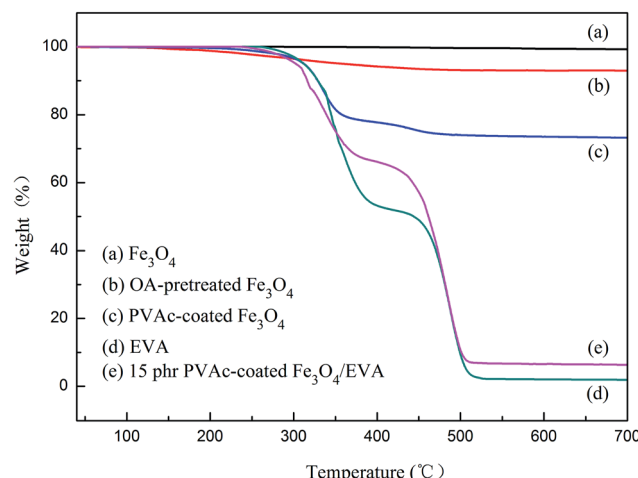
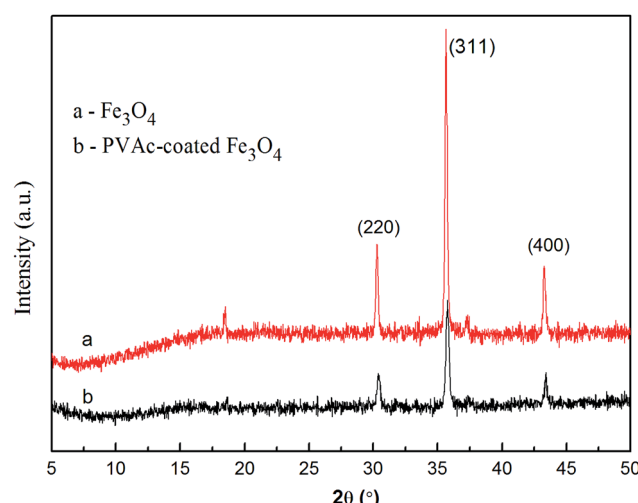
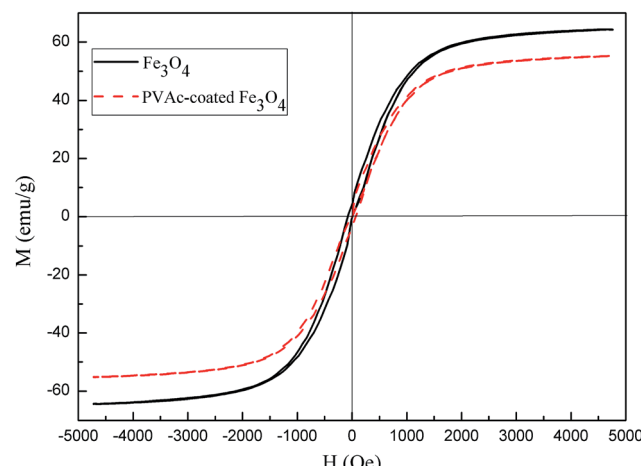


Fig. 4 TGA thermograms of magnetic particles and EVA HMAs.

particle size. Compared with EVA, for EVA adhesives with 15 phr of PVAc-coated  $\text{Fe}_3\text{O}_4$  particles, the weight retention rate just increased by 4.3% (Fig. 4), while the theoretical percentage of PVAc-coated  $\text{Fe}_3\text{O}_4$  particles in adhesives was 8.1%. Fig. 5 showed that both  $\text{Fe}_3\text{O}_4$  and the PVAc-coated  $\text{Fe}_3\text{O}_4$  presented strong diffraction peaks at  $30^\circ$ ,  $36^\circ$  and  $44^\circ$  corresponding to the crystal face (220), (311) and (400) of  $\text{Fe}_3\text{O}_4$ , respectively. The XRD result also indicated that the PVAc coating had no influence on the crystal structure of  $\text{Fe}_3\text{O}_4$ . The hysteresis curves (Fig. 6) showed that both  $\text{Fe}_3\text{O}_4$  and PVAc-coated  $\text{Fe}_3\text{O}_4$  particles were magnetic particles, but the magnetization intensity of PVAc-coated  $\text{Fe}_3\text{O}_4$  particles was lower than that of the  $\text{Fe}_3\text{O}_4$  particles. This may be because that the PVAc organic coating weakened the magnetization intensity of PVAc-coated  $\text{Fe}_3\text{O}_4$ .

### 3.2. Morphology observation

The morphology of different kinds of EVA composite HMAs was observed by SEM, as shown in Fig. 7. For the unmodified EVA

Fig. 5 X-ray diffractograms of  $\text{Fe}_3\text{O}_4$  and PVAc-coated  $\text{Fe}_3\text{O}_4$ .Fig. 6 Hysteresis curves of  $\text{Fe}_3\text{O}_4$  and PVAc surface coated  $\text{Fe}_3\text{O}_4$  particles.

composite HMAs (Fig. 7a), the morphology is homogeneous and the fracture morphology is smooth. For the  $\text{Fe}_3\text{O}_4$  modified EVA composite HMAs (Fig. 7b), however, there existed obvious phase separation.  $\text{Fe}_3\text{O}_4$  particles aggregate seriously in HMAs because of the magnetic force among  $\text{Fe}_3\text{O}_4$  particles as well as the poor compatibility of the inorganic  $\text{Fe}_3\text{O}_4$  particles with EVA matrix. For PVAc-coated  $\text{Fe}_3\text{O}_4$  modified EVA composite HMAs as shown in Fig. 7c, the aggregation was slightly reduced. The PVAc-coated particles dispersed better compared to the  $\text{Fe}_3\text{O}_4$  modified EVA composite HMAs (Fig. 7b). This is because, on one hand, the organic PVAc coating had good compatibility with EVA matrix, resulting in improved compatibility of PVAc-coated  $\text{Fe}_3\text{O}_4$  with EVA matrix. On the other hand, the organic PVAc coating weakened the magnetic intensity of PVAc-coated  $\text{Fe}_3\text{O}_4$  (Fig. 6), which could also hinder the aggregation of PVAc-coated  $\text{Fe}_3\text{O}_4$  in EVA matrix.

### 3.3. Peel strength

The relationship between the peel strength and the content of magnetic particles was shown in Fig. 8. The results clearly showed that, both for EVA and the EVA-g-MAH composite HMAs, adding magnetic particles could increase the peel strength, especially for the PVAc-coated  $\text{Fe}_3\text{O}_4$  particles. We previously showed that all the failure mode of EVA composite HMAs was interface failure, for that the adhesion property of HMAs was poor. Adding magnetic particles, especially the PVAc-coated  $\text{Fe}_3\text{O}_4$ , could improve the adhesion property as shown from the results of Fig. 8.

For EVA composite HMAs, the peel strength without magnetic particles was  $1.9 \text{ kN m}^{-1}$ , but increased by 89% to  $3.6 \text{ kN m}^{-1}$  when 15 phr of  $\text{Fe}_3\text{O}_4$  particles were added. The peel strength could be further increased by 247% to  $6.6 \text{ kN m}^{-1}$  when 15 phr of PVAc-coated  $\text{Fe}_3\text{O}_4$  particles were added (Fig. 8).

These were because, first, that both the  $\text{Fe}_3\text{O}_4$  and PVAc-coated  $\text{Fe}_3\text{O}_4$  had magnetic interaction with iron plate, and the magnetic force increased the peel strength of HMAs. Second, when HMAs were heated to melt during sample

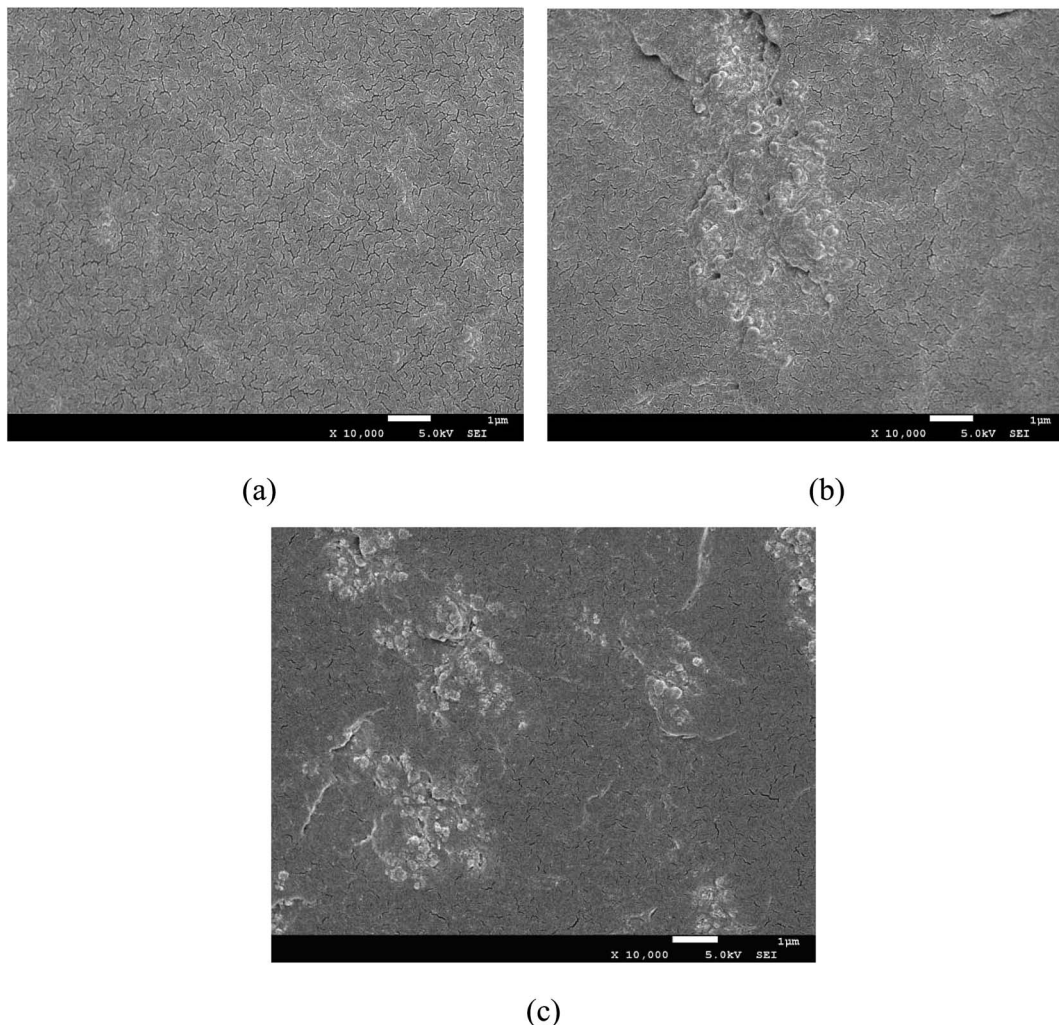


Fig. 7 SEM micrographs of cryogenically fractured surface of (a) EVA composite HMs; (b)  $\text{Fe}_3\text{O}_4$ /EVA composite HMs; (c) PVAc-coated  $\text{Fe}_3\text{O}_4$ /EVA composite HMs.

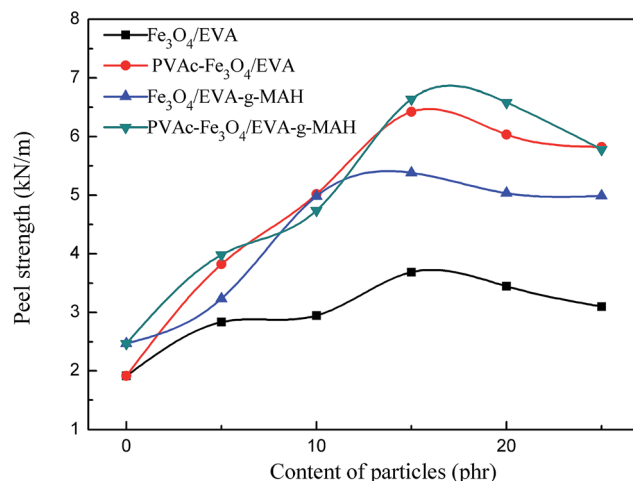


Fig. 8 Peel strength of different HMs with different content of particles.

preparation of peel test, magnetic particles could move towards the iron plate under magnetic force. At the same time, the polar vinyl acetate segments of EVA molecular were induced to follow the move due to the polar interaction between polar vinyl acetate segments and the organic PVAc coating of PVAc-coated  $\text{Fe}_3\text{O}_4$ . As a result, there were more polar segments on the iron plate side and more nonpolar segments on the PE plate side, which led to the increased adhesion of HMs with iron plate and PE plate. In addition, compared with the uncoated particles, PVAc-coated magnetic particles had better compatibility with EVA matrix. This could also enhance the movement of magnetic particles and further improve the adhesion property of HMs. It was noticed that the peel strength would begin to decrease if the content of magnetic particles was further increased, notably over 15 phr (Fig. 8). This is because that the magnetic particles content reached a critical point where they might aggregate more easily,<sup>18</sup> thus weakening the adhesion property.

Similarly, for EVA-g-MAH composite HMs, the peel strength showed the same trend but was higher than EVA composite

HMA in value (Fig. 8). This is because the polar MAH groups increased the polarity of HMA and reinforced the interaction with the polar iron plate.

### 3.4. Segments orientation of PVAc-coated $\text{Fe}_3\text{O}_4$ modified EVA composite HMA

The orientation structure of EVA chain segments could be revealed by infrared dichroism.<sup>22,23</sup> The broad peak at 2700–3000  $\text{cm}^{-1}$ , caused by the overlap between the stretching vibration peak and asymmetric stretching vibration peak of  $\text{CH}_2$  in EVA molecule,<sup>20</sup> was clearly seen (Fig. 9). The peak at about 720  $\text{cm}^{-1}$  was attributed to the in-plane bending vibration peak of  $\text{CH}_2$ .<sup>19</sup> The broad peak at 1600–1800  $\text{cm}^{-1}$  was the stretching vibration peak of  $\text{C}=\text{O}$ <sup>20,24</sup> and the peak at 1382–1443  $\text{cm}^{-1}$  was the in-plane bending vibration peak of  $\text{C}-\text{H}$ .<sup>19,20</sup>

To further study the orientation degree of EVA composite HMA with different particles content, the relative orientation degree of  $\text{CH}_2$  at 720  $\text{cm}^{-1}$  and  $\text{C}=\text{O}$  at 1742  $\text{cm}^{-1}$  was used to represent the orientation degree of EVA composite HMA. The relative orientation degree of both  $\text{CH}_2$  and  $\text{C}=\text{O}$  increased with the increased content of PVAc-coated  $\text{Fe}_3\text{O}_4$  particles (Fig. 10), indicating an increased orientation degree of the PVAc-coated  $\text{Fe}_3\text{O}_4$  modified EVA composite HMA. It was also found that the orientation degree of  $\text{C}=\text{O}$  was more obviously

increased and higher than that of the  $\text{CH}_2$  (Fig. 10). This is because the polar vinyl acetate segments of EVA had stronger interaction force with magnetic particles compared with the PE segments of EVA. When PVAc-coated  $\text{Fe}_3\text{O}_4$  particles moved towards the polar iron plate, more vinyl acetate segments were induced to facilitate the movement and orientation.

To study the relationship between peel strength and relative orientation degree, the relative orientation degree of  $\text{C}=\text{O}$  with test angle of (0, 90°) was used to represent the relative orientation degree of PVAc-coated  $\text{Fe}_3\text{O}_4$  modified EVA composite HMA. The result (Fig. 11) showed that the peel strength increased at first and then decreased with increased relative orientation degree. This indicated that the increase of orientation degree at certain extent could improve the peel strength. However, it (Fig. 11) was also found that, when the content of magnetic particles was over 15 phr, namely the relative orientation degree surpassed 13%, the orientation degree continued to increase but the peel strength decreased with the increased content of magnetic particles. This finding was in accordance with what was shown in Fig. 7. This is because, although an increased orientation degree of  $\text{C}=\text{O}$  reflects that more VA segments interacted with iron plate thus increased the peel strength, the peel strength can also be compromised by the poor dispersity of particles at relatively higher content.

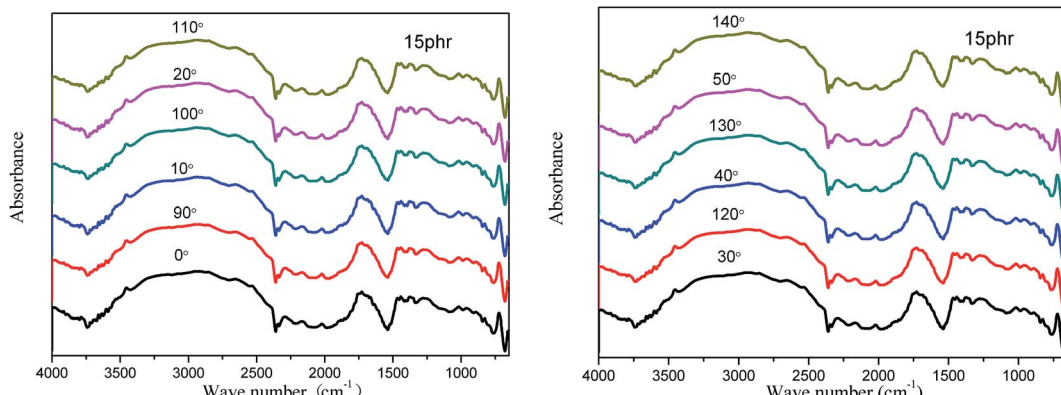


Fig. 9 Infrared dichroism spectra of EVA composite HMA with 15 phr of the PVAc-coated  $\text{Fe}_3\text{O}_4$  particles.

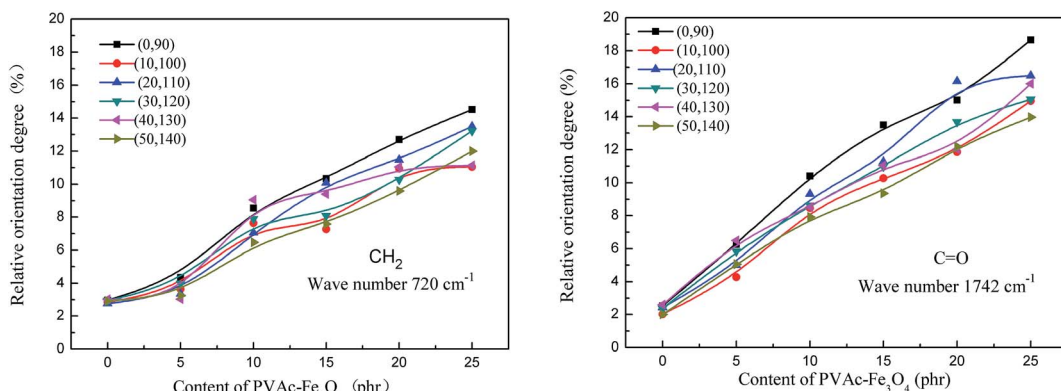


Fig. 10 Relative orientation degree of  $\text{CH}_2$  and  $\text{C}=\text{O}$ .



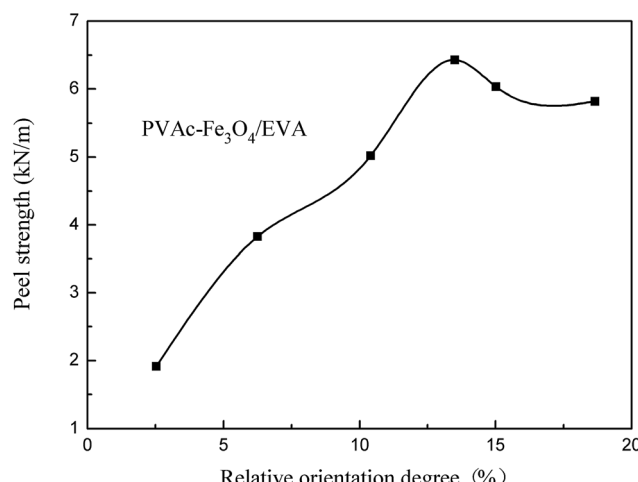


Fig. 11 The relationship between peel strength and relative orientation degree.

### 3.5. Water contact angle

When magnetic particles modified EVA composite HMsAs were used to bond iron plate and PE plate, the interfacial property of HMsAs with the two kinds of materials could be altered due to the interaction of magnetic particles with the iron plate. This is characteristic of a change in the water contact angle.

The water contact angle of composite HMsAs, both for the contact surfaces with iron plate and PE plate, all decreased accordingly after being modified respectively by  $\text{Fe}_3\text{O}_4$  and

Table 1 Interfacial contact angle of different kinds of EVA composite HMsAs

Sample	Contact angle (degree)	
	Contact surface with iron plate	Contact surface with PE plate
EVA	84.60	84.60
$\text{Fe}_3\text{O}_4$ /EVA	78.65	79.99
PVAc-coated $\text{Fe}_3\text{O}_4$ /EVA	67.88	73.36

PVAc-coated  $\text{Fe}_3\text{O}_4$  with the same 15 phr content (Table 1). The decreased water contact angle of HMsAs indicated improved wettability. The results (Table 1) showed that the PVAc-coated  $\text{Fe}_3\text{O}_4$  was better than the pristine  $\text{Fe}_3\text{O}_4$  at improving the wettability of EVA composite HMsAs, especially for iron plate.

### 3.6. Crystallization

The crystallinity of EVA composite HMsAs (Fig. 13) was determined from the DSC curves (Fig. 12). The relative crystallinity of EVA composite HMsAs obviously increased with the increased content of magnetic particles, however, it began to decrease for  $\text{Fe}_3\text{O}_4$  modified EVA composite HMsAs when the content of  $\text{Fe}_3\text{O}_4$  without PVAc coating was over 20 phr. The change is more significant for the PVAc-coated  $\text{Fe}_3\text{O}_4$  than for pristine  $\text{Fe}_3\text{O}_4$  (Fig. 13), indicating more influence on crystallinity of the former. It is worth to mention that PVAc-coated  $\text{Fe}_3\text{O}_4$  had better compatibility with HMsAs and could disperse better in HMsAs than  $\text{Fe}_3\text{O}_4$ . This made PVAc-coated  $\text{Fe}_3\text{O}_4$  move more easily in HMsAs thus reinforced the induced orientation effect of segments (Fig. 10), resulting in the increase of crystallinity. Other than that, the poor compatibility of  $\text{Fe}_3\text{O}_4$  with HMsAs made  $\text{Fe}_3\text{O}_4$  aggregate in HMsAs, which further restricted the segments motion and weakened the induced orientation movement of segments, leading to the decrease of crystallization ability.

### 3.7. Rheological property

The processing fluidity was an important parameter for HMsAs in application, because it not only affects the wettability to the bonding materials but also influences the coating performance. The result of rheological test, shown in Fig. 14, showed that the viscosity of EVA composite adhesives at low shear rate had little change and was often regarded as the zero shear viscosity. Compared with the unmodified EVA adhesives, both the zero shear viscosity of  $\text{Fe}_3\text{O}_4$  and the PVAc-coated  $\text{Fe}_3\text{O}_4$  modified EVA composite adhesives increased and their viscosity at high shear rate was changed more obviously (Fig. 14). These indicated that magnetic particles modified EVA composite HMsAs had better pseudoplastic behavior and processing fluidity than the unmodified HMsAs. The results also showed that, for the modified EVA composite HMsAs, adding 5 phr of magnetic

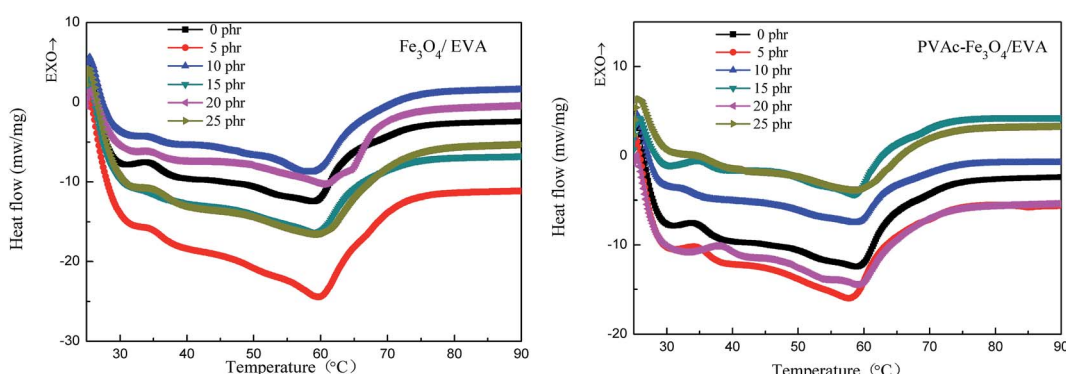


Fig. 12 DSC thermograms of  $\text{Fe}_3\text{O}_4$ /EVA and PVAc-coated  $\text{Fe}_3\text{O}_4$ /EVA composite HMsAs.

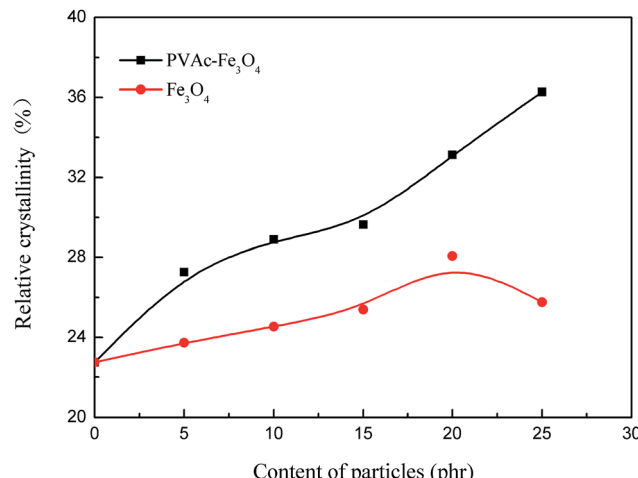


Fig. 13 Relative crystallinity of EVA composite HMAs with different content of  $\text{Fe}_3\text{O}_4$  and PVAc-coated  $\text{Fe}_3\text{O}_4$ .

particles led to the highest zero shear viscosity and presented the best pseudoplastic behavior at high shear rate. This is because moderate magnetic particles could induce segments of EVA to orient at high shear rate, consequently increased the orientation degree but decreased the viscosity at high shear rate according to the shear thinning theory.

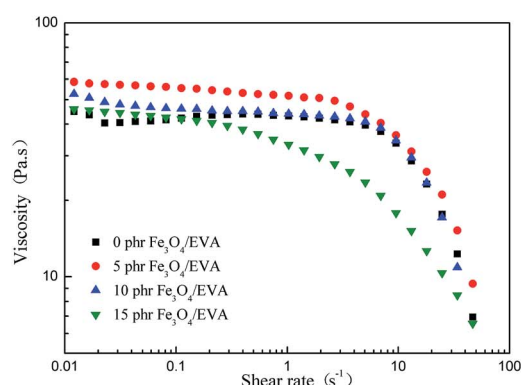


Fig. 14 Apparent viscosity of EVA composite HMAs with different content of  $\text{Fe}_3\text{O}_4$  and PVAc-coated  $\text{Fe}_3\text{O}_4$  at different shear rate.

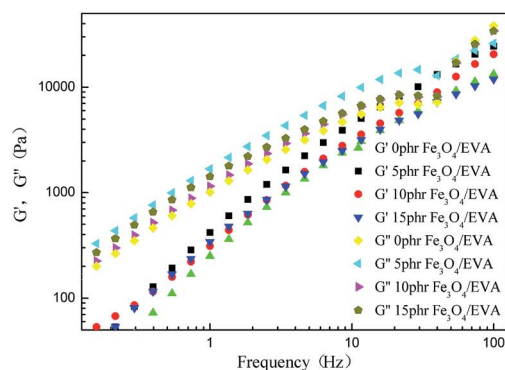


Fig. 15 Modulus of  $\text{Fe}_3\text{O}_4$  modified and PVAc-coated  $\text{Fe}_3\text{O}_4$  modified EVA composite HMAs at different frequency.

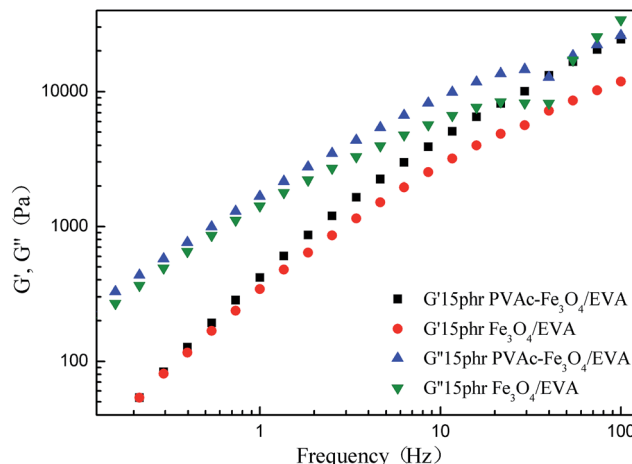
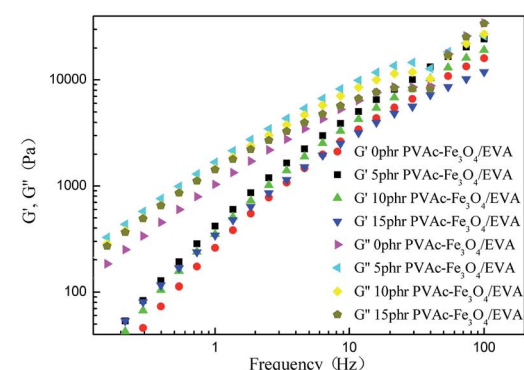
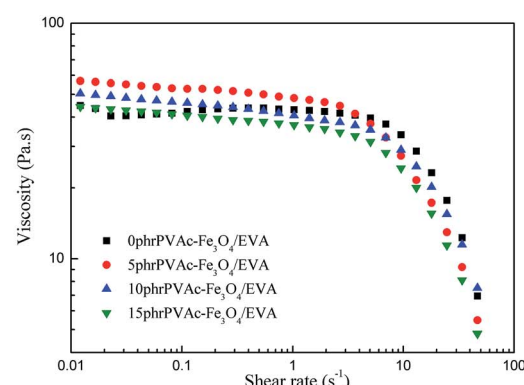


Fig. 16 Modulus of modified EVA composite HMAs with 15 phr  $\text{Fe}_3\text{O}_4$  or PVAc-coated  $\text{Fe}_3\text{O}_4$ .

For the  $\text{Fe}_3\text{O}_4$  modified and PVAc-coated  $\text{Fe}_3\text{O}_4$  modified EVA composite HMAs, both the storage modulus  $G'$  and loss modulus  $G''$  increased and were higher than the unmodified EVA composite HMAs (Fig. 15). It was found that PVAc-coated  $\text{Fe}_3\text{O}_4$  particles modified EVA composite HMAs had higher  $G'$  and  $G''$  than  $\text{Fe}_3\text{O}_4$  modified EVA composite HMAs (Fig. 16),



because of the better compatibility of PVAc-coated  $\text{Fe}_3\text{O}_4$  particles with EVA adhesives.

## 4. Conclusions

We have shown that when the magnetic  $\text{Fe}_3\text{O}_4$  particles were surface coated with a layer of PVAc polymer, the compatibility of magnetic  $\text{Fe}_3\text{O}_4$  particles with EVA adhesives could be improved with only a slight decrease in the magnetization intensity of the magnetic particles.

Adding PVAc-coated  $\text{Fe}_3\text{O}_4$  particles greatly improved the peel strength and adhesion property of EVA composite HMAs. For the modified HMAs with 15 phr of the PVAc-coated  $\text{Fe}_3\text{O}_4$  particles, the peel strength was increased by 247% to a value of  $6.6 \text{ kN m}^{-1}$  compared with the unmodified HMAs. The peel strength of the HMAs with PVAc-coated  $\text{Fe}_3\text{O}_4$  particles was also higher than the one without PVAc coating, with only  $3.6 \text{ kN m}^{-1}$  for the latter at  $\text{Fe}_3\text{O}_4$  particles of 15 phr. In addition, adding PVAc-coated  $\text{Fe}_3\text{O}_4$  magnetic particles also greatly enhanced the orientation and crystallization of EVA composite HMAs. PVAc-coated  $\text{Fe}_3\text{O}_4$  modified EVA composite HMAs presented better pseudoplastic behavior and processing fluidity than the unmodified EVA composite HMAs. This work adds to the body of knowledge to improve the adhesion property of HMAs containing  $\text{Fe}_3\text{O}_4$  particles.

## Acknowledgements

This work was financially supported by the State Key Laboratory of Oil and Gas Reservoir Geology and Exploitation of China (No. X151515KCL36); X. W. acknowledges a start-up funding from Southwest Petroleum University and a funding from the Education Department of Sichuan Province of China (No. 17ZA0419).

## References

- 1 H. Dahmane, *Int. J. Adhes. Adhes.*, 1996, **16**, 43–45.
- 2 R. D. Mitchell, *Adhes. Age*, 1999, **42**, 24–27.
- 3 R. Tout, *Int. J. Adhes. Adhes.*, 2000, **20**, 269–272.
- 4 M. Stolt, M. Viljanmaa, A. Södergård and P. Törmälä, *J. Appl. Polym. Sci.*, 2004, **91**, 196–204.
- 5 W. Li, L. Bouzidi and S. S. Narine, *Ind. Eng. Chem. Res.*, 2008, **47**, 7524–7532.
- 6 J. Schwartz, *Adhes. Age*, 2001, **44**, 7–10.
- 7 D. D. Gray, *Adhes. Age*, 1998, **41**, 23–24.
- 8 A. T. Hu, R. S. Tsai and Y. D. Lee, *J. Appl. Polym. Sci.*, 1989, **37**, 1863–1876.
- 9 N. R. Jarvis, *Adhes. Age*, 1995, **38**, 26–28.
- 10 M. L. Barrueso-Martinez, T. P. Ferrández-Gómez, M. D. Romero-Sánchez and J. M. Martín-Martínez, *J. Adhes.*, 2003, **79**, 805–824.
- 11 Y. X. Wu and C. X. Shen, *Chem. Adhes.*, 2006, **28**, 166–168.
- 12 J. P. Qiao, *Corros. Prot.*, 2007, **28**, 590–593.
- 13 M. Takemoto, M. Kajiyama, H. Mizumachi, A. Takemura and H. Ono, *J. Appl. Polym. Sci.*, 2002, **83**, 719–725.
- 14 M. Takemoto, M. Kajiyama, H. Mizumachi, A. Takemura and H. Ono, *J. Appl. Polym. Sci.*, 2002, **83**, 726–735.
- 15 Y. J. Park and H. J. Kim, *Int. J. Adhes. Adhes.*, 2003, **23**, 383–392.
- 16 Y. J. Park, H. J. Kim, M. Rafailovich and J. Sokolov, *J. Adhes. Sci. Technol.*, 2003, **17**, 1831–1845.
- 17 X. R. He, R. Zhang and S. Hui, *China Plast. Ind.*, 2013, **41**, 49–52.
- 18 X. R. He, R. Zhang, C. Y. Yang, Y. Q. Rong and G. S. Huang, *Int. J. Adhes. Adhes.*, 2013, **44**, 9–14.
- 19 X. R. He, R. Zhang, Q. Chen, Y. Q. Rong and Z. Q. Yang, *Int. J. Adhes. Adhes.*, 2014, **50**, 128–135.
- 20 X. R. He, X. B. Lu, Q. Chen and R. Zhang, *J. Appl. Polym. Sci.*, 2016, **133**, DOI: 10.1002/app.43931.
- 21 R. J. Samuels, *Macromol. Chem. Phys.*, 1981, **4**, 241–270.
- 22 T. Kimura, H. Ago, M. Tobita, S. Ohshima, M. Kyotani and M. Yumura, *Adv. Mater.*, 2002, **14**, 1380–1383.
- 23 Y. P. Rodin, *Mech. Compos. Mater.*, 1991, **27**, 331–343.
- 24 E. Wisse, A. J. H. Spiering, F. Pfeifer, G. Portale, H. W. Siesler and E. W. Meijer, *Macromolecules*, 2009, **2**, 524–530.

